DEVELOPMENT AND APPLICATION OF AN EMPIRICAL PROBABILITY DISTRIBUTION FOR THE PREDICTION ERROR OF RE-ENTRY BODY MAXIMUM DYNAMIC PRESSURE

R. James Lanzi
National Aeronautics and Space Administration
Goddard Space Flight Center
Wallops Flight Facility
Wallops Island, VA 23337

Brett T. Vincent
Computer Sciences Corporation
Wallops Flight Facility
Wallops Island, VA 23337

ABSTRACT

The relationship between actual and predicted re-entry maximum dynamic pressure is characterized using a probability density function and a cumulative distribution function derived from sounding rocket flight data. This paper explores the properties of this distribution and demonstrates applications of this data with observed sounding rocket re-entry body damage characteristics to assess probabilities of sustaining various levels of heating damage. The results from this paper effectively bridge the gap existing in sounding rocket re-entry analysis between the known damage level/flight environment relationships and the predicted flight environment.

1.0 INTRODUCTION

Figure 1 shows a schematic of a typical re-entry configuration for a Terrier-Black Brant sounding rocket payload. Historically at NASA/GSFC/Wallops Flight Facility, 5 degree-of-freedom trajectory simulations (Reference 1) have been used to predict sounding rocket re-entry body flight environment parameters such as maximum dynamic pressure, Mach 1 altitude and parachute deployment conditions. The aerodynamic characteristics used in these simulations have been computed using the CDCG computer program which incorporates a hybrid theoretical / empirical nonlinear crossflow aerodynamics model.

As the NASA Sounding Rocket Program has shifted toward larger payload size and increased vehicle performance capability, concern over aerodynamic heating during re-entry has become more than just an academic issue. Re-entry heating damage to sounding rocket recovery systems has been a source of refurbishment cost, and a cause for apprehension over possible recovery system failure. The level of heating damaged sustained by any given

sounding rocket payload during the re-entry leg of the flight has been found to be directly related to the peak level of dynamic pressure encountered and the static margin of the re-entry body. A crude characterization of the relationship between the aerodynamic heating damage and maximum dynamic pressure was determined in Reference 2. In this report, a "damage line" is defined which separates values of flight dynamic pressure and re-entry body static margin that constitute a "cool region", within which no heating damage has been experienced, from values of flight dynamic pressure and static margin which constitute a "hot" region where varying degrees of heating damage have been experienced.

Flight levels of maximum dynamic pressure can vary significantly from the predicted values. In Reference 2, the limitations of the analysis tools used to make predictions of the re-entry environment parameters were investigated, and several sources of prediction error were isolated. In particular, a statistical characterization of the prediction error in the aerodynamic properties was determined.

Before the study of Reference 2, NASA/GSFC/Wallops Flight Facility imposed a fixed limit on predicted maximum dynamic pressure to prevent recovery system failure due to re-entry heating. Payloads were ballasted to meet this constraint. Once the study of Reference 2 was published, NASA began using the observed properties of the prediction error of re-entry body aerodynamic characteristics to analytically determine the dispersion of re-entry environment parameters such as maximum dynamic pressure (q_{max}) and Mach 1 altitude (References 2 and 3). Re-entry bodies are then ballasted to bring the envelope of predicted levels of maximum dynamic pressure beneath the "damage line" given in Reference 2. Although this technique does address the variability in predicted re-entry dynamic pressure levels, the inherent noise involved in the determination of the prediction error of the body aerodynamics combined with the extreme sensitivity of the re-entry environment to variations in body aerodynamic characteristics makes it difficult to interpret the results from this approach.

During the post flight mission analyses of Terrier-Black Brant V Flights 36.079 and 36.089 it was observed that the predicted re-entry maximum dynamic pressures (q_p) were 20.2% and 15.3% lower, respectively, than the actual re-entry maximum dynamic pressures (q_a). Flight 36.089 was a refly of the 36.079 payload. Further analysis revealed that there was an apparent center of pressure shift away from the S-19 canards for both flights. Reference 2 noted that for the 28 analyzed cases, the apparent center of pressure shift was towards the S-19 canards. Approximately 9 Lbs. of re-entry ballast were incorporated on these flights to bring q_p below the "damage line" of Reference 2. These flights illustrate the difficulty in applying the results of Reference 2 to payload ballast design.

In this report, the direct statistical relationships between predicted and actual maximum dynamic pressure are developed, and the relationship between re-entry heating damage and maximum dynamic pressure is refined. These results are combined into a coherent method for relating results from simulation to probability of sustaining various levels of aerodynamic heating damage during re-entry.

2.0 CHARACTERISTICS OF RE-ENTRY ENVIRONMENT PREDICTION ERROR

2.1 Prediction Error Determination

The re-entry environment prediction error is characterized by the percent error in predicting q_a ($\%q_{err}$), which is given by:

$$\%q_{err} = (\frac{q_p - q_a}{q_a}) * 100\%. \tag{1}$$

The percent error was determined for the 49 flights listed in Table 1. As was done in References 2 and 4, q_p was determined by initializing a GEM 5-DOF re-entry simulation (containing nonlinear aerodynamics from the CDCG program) with radar data at some time prior to re-entry. This was done to eliminate trajectory dispersion effects.

2.2 Generation of an Empirical Probability Density Function

It can be seen in Table 1 that $\%q_{err}$ varies widely, from -54.5% to +232.5%. However, closer inspection of the data reveals that the majority of cases fall within ±30% error range. A distribution for $\%q_{err}$ was determined by generating a normalized relative frequency histogram h(x); that is, dividing the $\%q_{err}$ values into 10 $\%q_{err}$ class intervals and determining the frequency of $\%q_{err}$ values within each interval. The intervals are represented mathematically by

$$[c_0, c_1), \ [c_1, c_2), \ ..., \ [c_{k-1}, c_k),$$

where k is the number of class intervals (10 in this case). The above notation denotes that the class intervals are closed on the left; that is, a value on a boundary point is assigned to the class interval that has this value as its lower boundary. The interval widths were chosen

to give a more or less continuous distribution. The normalized relative frequency histogram is defined by

$$h(x) = \frac{f_i/n}{c_i - c_{i-1}} \quad for \ c_{i-1} \le x \ c_i, \quad i=1,2,...,10, \tag{2}$$

where n is the number of observations and f_i is the frequency of the class $[c_{i-1}, c_i)$. The normalized relative frequency histogram is an approximation of the probability density function for $\%q_{err}$. Probability values for the event that a random variable, x, falls within a certain interval are given by the area beneath the probability density function, f(x), over the interval. Figure 2 presents the normalized relative frequency histogram for the $\%q_{err}$ of the 49 subject cases. As was observed in Table 1, the distribution of $\%q_{err}$ is skewed to the right with the majority of cases being between $\pm 30\%$.

The relative frequency of an interval [a, b), where $c_0 \le a < b \le c_k$, can be computed by the integral

$$\int_a^b h(x)dx.$$

Since the relative frequency is an approximation to probability, this integral can be thought of as an approximation to the probability that X, the random variable under consideration ($\%q_{err}$), is in the interval [a, b). It follows that a cumulative distribution function F(x) can be derived from

$$F(x) = P(X \le x) = P(X < x) = \int_{-\infty}^{x} f(w)dw, \tag{3}$$

where f(x) is the limit of h(x) as n increases and the lengths of the class intervals go to zero.

2.3 Discussion of the Cumulative Distribution Function

The cumulative distribution function (c.d.f.) in Equation 3 gives the probability of having a value of the variable X (in this case, $\%q_{err}$) less than some given value x. Figure 3 presents the c.d.f. for $\%q_{err}$. The c.d.f. shows that while there is a 47.7% probability of

having a negative $\%q_{err}$ (that is, q_a greater than q_p), there have been no recorded cases of $\%q_{err}$ exceeding -60%. Qualitatively, the c.d.f. shows that most of the time the re-entry q_{max} prediction is fairly accurate, and is about as likely to be under the flight value as it is over, but the over predictions are of a much larger magnitude than the under predictions. Of course, it is the under predictions of re-entry q_{max} that are of greater concern, in terms of re-entry heating damage.

3.0 COMPUTING DAMAGE RISK USING THE EMPIRICAL ERROR DISTRIBUTION

Figure 4 shows the re-entry flight envelope of maximum dynamic pressure and re-entry static margin for the Terrier-Black Brant V family. The different symbols on the plot represent the different levels of heating damage sustained during the flight according to the following classifications:

Re-entry Heating Damage Classifications

0 - No damage. (36.096)

1 - Exterior discoloration. (36.053)

2 - Minor exterior erosion, especially near surface
  discontinuities. (36.049)

3 - Melting at surface discontinuities and erosion making
  its way into interior. (36.034)

4 - Major exterior damage. Skin eroding and peeling away
  from joint. (36.057)

5 - All above exterior damage plus significant interior
  damage. (36.086) .

6 - Failure due to re-entry heating (no known cases)

The lower line in Figure 4 separates the region in the flight envelope of Level 0 and 1 heating damage from the region of Level 2 and 3 heating damage. This line was previously published in Reference 2 and is given by the equation

$$q_{max}^{(1)} \leq 4200 - 17.5 * SM^2,$$ (4)

where

q_{max} = Flight maximum dynamic pressure (psf)

SM = $|xcg - xcla|$ (% Total Body Length).

The upper line in Figure 4 separates the Level 2/3 region from the higher level heating damage regions in the flight envelope. This line is defined by several borderline flights and is given by the equation

$$q_{max}^{(2)} \leq 4600 - 10.5 * SM^2.$$ (5)

For a re-entry body with a fixed static margin, values of $q_{max}^{(1)}$ and $q_{max}^{(2)}$ can be computed using Equations 4 and 5. A value of q_p is determined using the nonlinear aerodynamics of the CDCG program and the GEM 5-DOF simulation. At this point the probability of falling into the three regions of the flight envelope can be computed using the cumulative distribution function derived in Section 2.2. This is done as follows:

1.   Calculate the prediction errors associated with flight values of maximum dynamic pressure equal to $q_{max}^{(1)}$ and $q_{max}^{(2)}$:

$$\%q_{err}^{(1)} = \frac{q_p - q_{max}^{(1)}}{q_{max}^{(1)}} * 100\%$$

$$\%q_{err}^{(2)} = \frac{q_p - q_{max}^{(2)}}{q_{max}^{(2)}} * 100\%$$

2.   Compute the following probability values from the cumulative distribution curve (CDF) of Section 2.2:

$$p_1 = 1 - CDF(\%q_{err}^{(1)})$$

$$p_2 = CDF(\%q_{err}^{(2)})$$

$$p_3 = 1 - p_1 - p_2$$

where

p_1 = Probability of flight q_{max} (q_a) falling into the level 0/1 region.

p_2 = Probability of q_a falling into the higher level damage region (3/4/5/6).

p_3 = Probability of q_a falling into the level 2/3 damage region.

The procedure outlined above has been automated in a FORTRAN program called REPROB. The damage demarcation curves and the empirical cumulative distribution function will be updated as new cases are added to the re-entry database.

CONCLUSIONS

An empirical probability density function describing the re-entry environment prediction error has been derived by comparing predicted re-entry maximum dynamic pressure (q_p) to flight maximum dynamic pressure (q_a) for 49 flights. From this, a cumulative distribution function has been generated relating q_p to q_a; allowing the mission analyst to predict, to a given probability, if q_a will be in a possible heating damage region. The re-entry error distribution and the damage region definitions can easily be updated as new cases are flown and as previous flight data is found.

The methods given in this report utilize the properties of the re-entry environment prediction error to give a more direct means of assessing possible re-entry heating difficulties. Future work in refining the aerodynamic models should address the effect of changes on the prediction error distribution.

REFERENCES

1. 841.1 Wallops Flight Facility Computer Programs:
   WFF CDCG - Crossflow Drag Computer Program
   WFF GEM - 6-DOF Simulation Program
2. Lanzi, R. J.: A Quantitative Evaluation of the Mission Analysis Tools Used for the Prediction of Reentry Body Aerodynamic Characteristics and Reentry Trajectory Parameters. NASA Internal Memo, 9/91.
3. Lanzi, R. J.: A Procedure for the Determination of Sensitivities of Reentry Trajectory Predictions with Known Error Bands in Predicted Aerodynamic Coefficients. NASA Internal Memo, 12/91.

4. Vincent, B. T.: Preliminary Findings of the Comparison Between the Current CDC Code and a Modified CDC Code (CDCG) With Flight Data. CSC Memorandum, November 30, 1990.

5. Hogg, R. V.; Ledolter, J.: Engineering Statistics. Macmillan Publishing Co., 1987.

STATION
(in. TNT)

0.00 ——

35.66 ——

54.20 ——
56.70 ——

78.70 ——

87.20 ——

94.65 ——

106.65 —— ——← 17.26"

120.84 ——

(CG) 127.62 ——

135.84 ——
137.09 ——
(CLA) 138.76 ——

152.13 ——

163.39 ——
166.59 ——
167.84 ——

←—— 18.26"

233.84 ——
238.71 ——
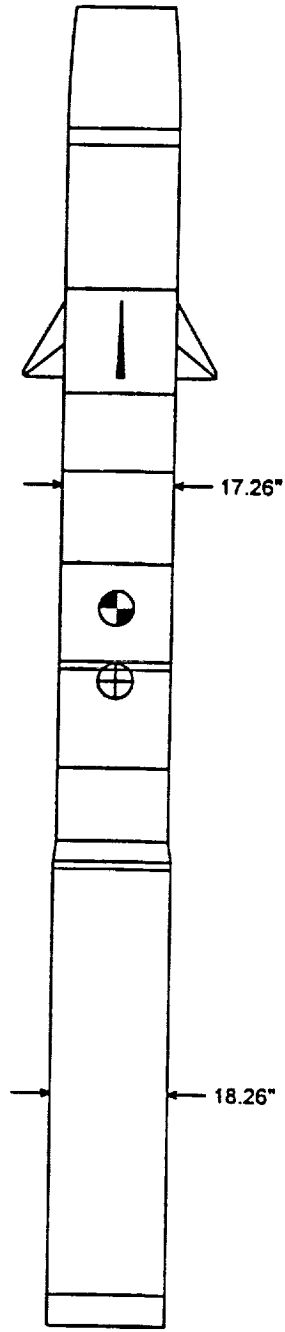
RE-ENTRY GRAVIMETRICS

Weight	=	875.00	lbs.
Length	=	203.05	in.
CG	=	127.62	in. TNT
CLA	=	138.76	in. TNT
[CG-CLA]	=	11.14	in.
I_x	=	8.61	slug-ft^2
I_y	=	665.47	slug-ft^2

Figure 1. Terrier - Black Brant VC 36.068 GG
Re-entry Configuration

277

Table 1. CDCG Comparison with Flight Data

Flight	Pred. Qmax	Flight Qmax	%Qerr
27.075	3565.6	2481.5	43.69%
27.106	2502.1	3071.5	-18.54%
27.121	2599.4	781.7	232.53%
27.122	945.6	821.0	15.17%
27.123	1888.3	1317.0	43.38%
27.124	2335.9	2388.0	-2.18%
27.129	1057.0	1116.0	-5.29%
27.130	1160.0	894.0	29.75%
27.133	1056.5	305.5	245.83%
36.016	2305.0	5061.6	-54.46%
36.025	3740.1	4271.6	-12.44%
36.027	١2703.4	1505.4	79.58%
36.030	2616.5	4103.5	-36.24%
36.032	2609.4	3090.7	-15.57%
36.034	2067.7	4110.0	-49.69%
36.035	3317.0	2673.2	24.08%
36.041	2874.5	3778.3	-23.92%
36.043	2730.0	1408.5	93.82%
36.047	1808.0	1230.9	46.88%
36.048	2800.0	2700.0	3.70%
36.049	3607.7	4334.9	-16.78%
36.052	1536.0	919.4	67.07%
36.053	1965.0	2938.5	-33.13%
36.054	1635.0	2344.1	-30.25%
36.057	4949.0	4739.7	4.42%
36.058	4643.0	4285.0	8.35%
36.059	2749.9	1277.2	115.31%
36.060	1633.0	622.2	162.46%
36.062	3958.0	4744.6	-16.58%
36.063	2342.0	3888.7	-39.77%
36.066	3383.1	3760.3	-10.03%
36.067	2715.3	1946.0	39.53%
36.068	4907.0	5238.2	-6.32%
36.069	3443.3	3352.5	2.71%
36.070	3365.0	3701.2	-9.08%
36.072	1916.3	1888.9	1.45%
36.073	4964.0	4267.6	16.32%
36.074	3146.4	2608.9	20.60%
36.077	5020.6	3268.3	53.62%
36.078	4584.0	4341.1	5.60%
36.079	3794.8	4757.0	-20.23%
36.085	4190.0	4230.0	-0.95%
36.086	4919.0	4413.5	11.45%
36.087	3153.2	3500.0	-9.91%
36.088	2124.7	2600.0	-18.28%
36.089	3921.0	4631.0	-15.33%
36.090	3800.0	3940.0	-3.55%
36.096	1907.7	812.7	134.74%
36.098	2740.0	2740.0	0.00%

RE-ENTRY BODY DYNAMIC PRESSURE PREDICTION ERROR
Normalized Relative Frequency Histogram
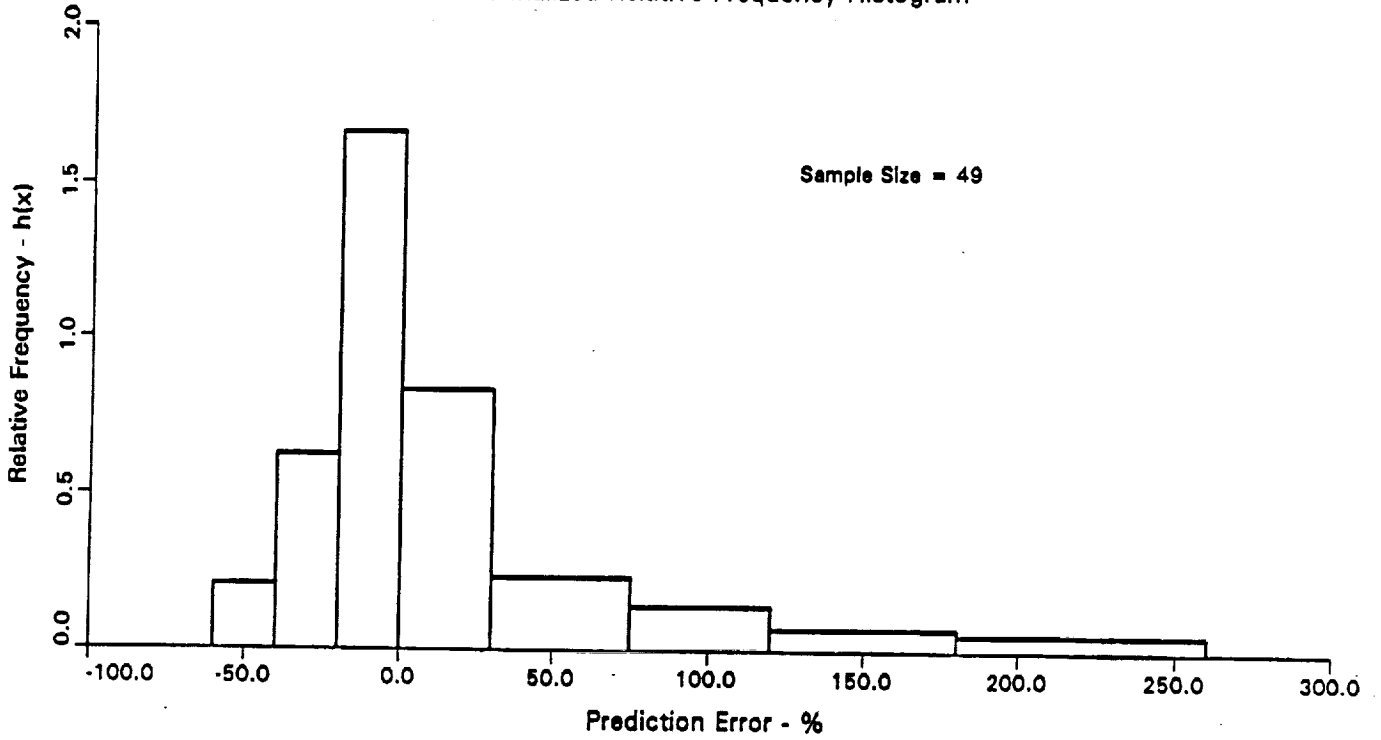
Figure 2

RE-ENTRY BODY DYNAMIC PRESSURE PREDICTION ERROR
Cumulative Distribution Function

Figure 3

279
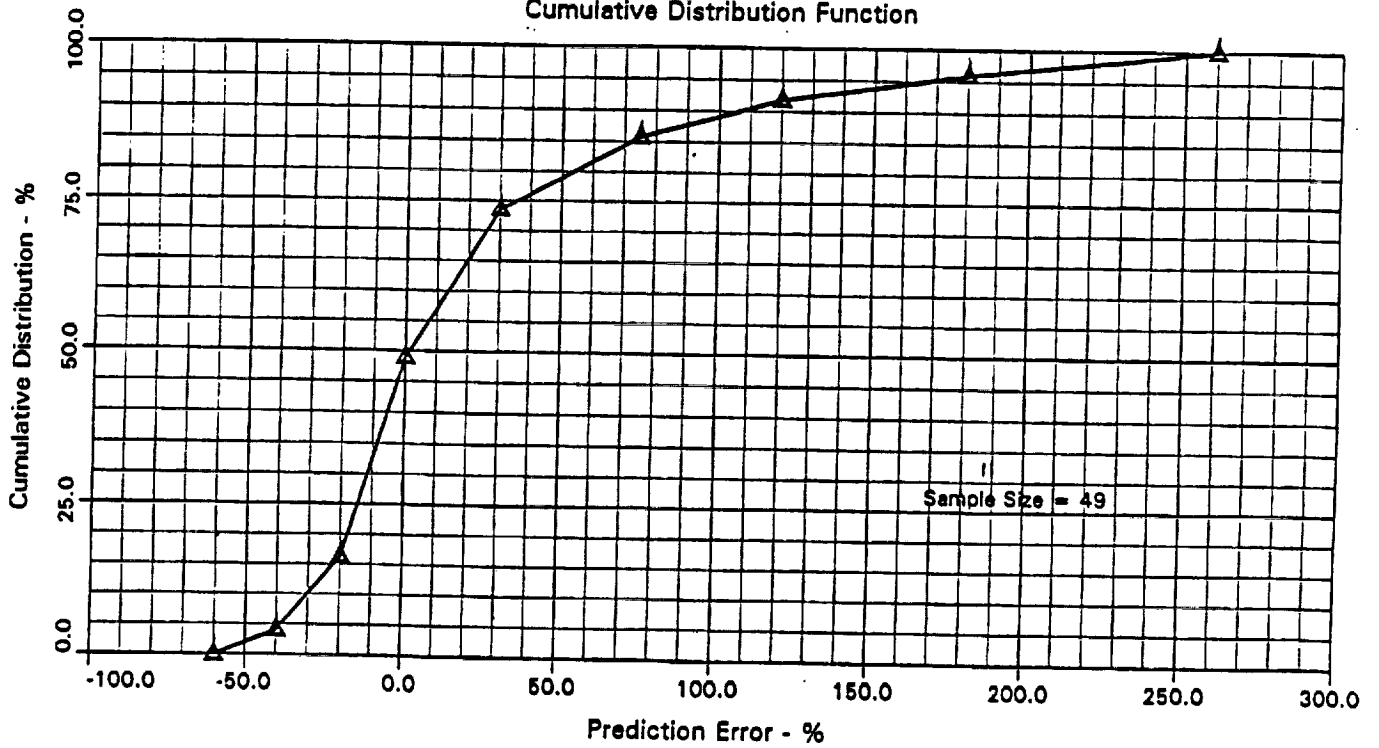
Terrier-Brant Reentry Study
Qmax vs SM

Figure 4